Mathematical Modelling and Control

https://www.aimspress.com/journal/mmc

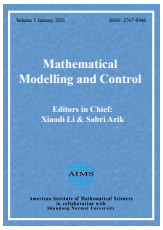

MMC, 5(3): 280–291.
DOI: 10.3934/mmc.2025019
Received: 16 October 2024
Revised: 06 March 2025
Accepted: 10 March 2025
Published: 24 July 2025

Research article

A practically stable explicit numerical method for the ternary Cahn–Hilliard system

Seokjun Ham[1], **Hyundong Kim**[2,3], **Youngjin Hwang**[1] **and Junseok Kim**[1,*]

[1] Department of Mathematics, Korea University, Seoul 02841, Republic of Korea

[2] Department of Mathematics and Physics, Gangneung-Wonju National University, Gangneung 25457, Republic of Korea

[3] Institute for Smart Infrastructure, Gangneung-Wonju National University, Gangneung 25457, Republic of Korea

* **Correspondence:** Email: cfdkim@korea.ac.kr.

Abstract: We propose a practically stable explicit finite difference method (FDM) for the ternary Cahn–Hilliard (CH) system, which involves challenging fourth-order nonlinear terms. Therefore, if we use a fully explicit numerical method such as the explicit Euler scheme, then the excessively restrictive time-step limitation makes it impractical to use. The proposed algorithm is based on the alternating direction explicit (ADE) scheme, which ensures both simplicity of implementation and stability of the computational solutions for the ternary CH system. To show the high performance of the proposed algorithm, we present multiple numerical experiments. The numerical tests demonstrate that the proposed method overcomes the stringent time-step limitations inherent in the explicit Euler method.

Keywords: ternary Cahn–Hilliard system; finite difference method; stable explicit numerical method; alternating directional explicit scheme

1. Introduction

The ternary Cahn–Hilliard (CH) system was proposed by Morral and Cahn [1] to model spinodal decomposition in three-component alloys. The ternary CH system can be used for materials science and phase separation studies by capturing complex phase behavior in materials with three distinct components to design and understand advanced materials [2]. The mathematical equations in the ternary CH system involve challenging fourth-order nonlinear terms, which describe intricate phenomena such as domain coarsening [3] and pattern formation [4]. Park [5] expanded the binary phase field model to a ternary model by extending a fourth-order free energy function. Researchers use the ternary CH system to explore and predict material properties, informing the development of new materials with tailored structures and functionalities. Consequently, its study enhances our ability to engineer materials for diverse applications in fields ranging from physics and chemistry to engineering and biology. Numerical algorithms are essential for solving the ternary CH system due to its complex nature and lack of analytical solutions. These methods enable efficient approximation, providing insights into phase separation phenomena and helping in understanding important materials science and physics phenomena. While a simple numerical method like explicit Euler is easy to implement, it becomes impractical for solving the ternary CH system due to stringent time step constraints. Implicit methods are preferred for effectively solving the challenges associated with the ternary CH system. Lee et al. [6] developed a high-order convex splitting method for a vector-valued CH system, which has three components, with nonlinearly coupled phase variables. Chen et al. [7] presented an unconditionally energy stable

numerical algorithm with Fourier pseudo-spectral method and convex splitting for the ternary CH system. Chen et al. [8] proposed an unconditionally stable method for the ternary CH type phase-field model for tri-block copolymers by using the scalar auxiliary variable method. Dong et al. [9] presented a positivity preserving and unconditionally energy stable finite difference method (FDM) for ternary CH system with a Flory–Huggins–de Gennes free energy potential. The developed method was theoretically analyzed by them for the uniqueness of the solution and its unconditional energy stability. Wang et al. [10] presented a time-marching method based on a combination of the projection algorithm and the invariant energy quadratization scheme to solve the ternary CH system and achieved linear and second-order accuracy in time

In addition, the ternary CH system can be applied in fluids. Rohde and Wolff [11] proposed a phase-field approach that couples Navier–Stokes equations with solid's ion concentration transportation with the ternary CH system. Zhan et al. [12] developed a ternary phase-field model for two-phase fluid flows in complex geometries by integrating a single CH equation with degenerate mobility and modified Navier–Stokes equations. A demonstration on fundamental conservation constraints, the second law of thermodynamics and vanishing interfacial width was given in the study. Manzanero et al. [13] presented how the three-component CH system can be used to model polymer blends at a continuum scale. The authors demonstrated the Gibbs free energy and showed that it is central in formulating a well-posed model, and provided various thermodynamic models. The ternary CH system can be expanded to the general multi-component system [14]. Multi-component CH system with singular potentials was studied by Gal et al. [15]. The authors of this study proved the well-posedness and the regularity of the system of nonlinear diffusion equations that model phase segregation of ideal mixture of multiple components. Zhou and Xie [16] presented a projected gradient method to simulate a multi-component CH equation. Li et al. [17] proposed unconditionally stable direct discretization schemes for the N-component CH system on curved surfaces.

The primary purpose of this article is to propose a stable FDM using an alternating direction explicit (ADE) scheme for solving the ternary CH system. The ADE scheme proposed by [18, 19] is an unconditionally stable explicit scheme. The diffusion and biharmonic terms, which are linear, can be solved with stability using the ADE scheme. For the nonlinear fourth-order CH equation, while unconditional stability is not guaranteed, it exhibits practical stability. The diffusion term can be discretized using isotropic finite difference discretization. This scheme not only relaxes the stringent time step requirement [20] but also effectively simulates phase separation [21] in both regular and complex computational domains, and under various boundary conditions [22, 23]. We should note that for a complex domain, an efficient discontinuous Galerkin method, such as the one developed and rigorously analyzed for the stochastic AC equation with multiplicative noise, can be applied [21].

The structure of this paper is as follows: In Section 2, we present the ternary CH system. In Section 3, the computational solution method is described. In Section 4, the computational experiments are given. We conclude the paper in Section 5.

2. Ternary Cahn–Hilliard system

We consider the following ternary CH system [24]:

$$\frac{\partial c_k(\mathbf{x},t)}{\partial t} = \Delta\mu_k(\mathbf{x},t), \quad \text{for } \mathbf{x}\in\Omega, \tag{2.1}$$

$$\mu_k(\mathbf{x},t) = F'(c_k(\mathbf{x},t)) - \epsilon^2\Delta c_k(\mathbf{x},t) + \beta(\mathbf{c}(\mathbf{x},t)), \quad \text{for} \quad k=1,2,3, \tag{2.2}$$

where $F'(c_k) = c_k^3 - 1.5c_k^2 + 0.5c_k$ and $\beta(\mathbf{c}) = -\sum_{k=1}^{3} F'(c_k)/3$. Here, ϵ is a positive constant and $\mathbf{c}(\mathbf{x},t) = (c_1(\mathbf{x},t), c_2(\mathbf{x},t), c_3(\mathbf{x},t))$ is ternary phase variable with the constraint $c_1 + c_2 + c_3 = 1$, $\mathbf{c} \in G_s$, where

$$G_s = \left\{ \mathbf{c}\in\mathbb{R}^3 \,\middle|\, \sum_{k=1}^{3} c_k = 1,\ 0\le c_k\le 1, \text{ for } k=1,2,3 \right\}.$$

Here, we use the following total free energy functional of the ternary system on a domain Ω.

$$\mathcal{E}(\mathbf{c}(\mathbf{x},t)) = \int_\Omega \left(\sum_{k=1}^{3} F(c_k(\mathbf{x},t)) + \frac{\epsilon^2}{2}\sum_{k=1}^{3} |\nabla c_k(\mathbf{x},t)|^2 \right) d\mathbf{x},$$

which satisfies energy dissipation

$$\frac{d}{dt}\mathcal{E}(\mathbf{c}) = -\int_\Omega \sum_{k=1}^{3} |\nabla\mu|^2 d\mathbf{x} \le 0,$$

and the governing system satisfies mass conservation

$$\frac{d}{dt}\int_\Omega c_k d\mathbf{x} = \int_\Omega \frac{\partial c_k}{\partial t} d\mathbf{x} = \int_\Omega \Delta\mu_k d\mathbf{x} = 0,$$

under the zero Neumann boundary condition [25]:

$$\mathbf{n}\cdot\nabla c_k = \mathbf{n}\cdot\nabla\mu_k = 0, \quad \text{on } \partial\Omega.$$

3. Computational method

We present the discrete numerical solution algorithms for solving the CH system. We consider the ternary CH system in $\Omega = (L_x, R_x)\times(L_y, R_y)$. We set the uniform grid size $h = (R_x - L_x)/N_x = (R_y - Ly)/N_y$, where N_x and N_y are the number of grid points for the x- and y-directions, respectively. To discretize the domain, Ω is divided into square cells with side length h, and each of these squares is defined as a cell. We define $\Omega_h = \{(x_p = L_x + h(p-0.5), y_q = L_y + h(q-0.5)) | 1 \le p \le N_x,\ 1 \le q \le N_y\}$, which is the set of cell-centers. Let $c^n_{k,p,q} = c_k(x_p, y_q, n\Delta t)$, where Δt is the uniform time step size. Then, we discretize the ternary CH system (Eqs (2.1) and (2.2)) using the linear convex splitting scheme [26]:

$$\begin{aligned}\frac{c^{n+1}_{k,p,q} - c^n_{k,p,q}}{\Delta t} &= \Delta_d((c^n_{k,p,q})^3 - \tfrac{3}{2}(c^n_{k,p,q})^2) + \tfrac{1}{2}\Delta_d c^{n+1}_{k,p,q} \\ &\quad -\epsilon^2\Delta_d^2 c^{n+1}_{k,p,q} + \Delta_d\beta(\mathbf{c}^n_{k,p,q}),\end{aligned} \tag{3.1}$$

where $\beta(\mathbf{c}^n_{k,p,q}) = -\sum_{k=1}^3 [(c^n_{k,p,q})^3 - 1.5(c^n_{k,p,q})^2 + 0.5c^n_{k,p,q}]/3$. Discrete Laplacian and biharmonic operators are defined as $\Delta_d c_{k,p,q} = (c_{k,p+1,q} + c_{k,p-1,q} + c_{k,p,q+1} + c_{k,p,q-1} - 4c_{k,p,q})/h^2$ and $\Delta_d^2 c_{k,p,q} = \Delta_d(\Delta_d c_{k,p,q})$, respectively. Zero Neumann boundary condition [27] is used as follows:

$$c^n_{k,p,-1} = c^n_{k,p,2}, c^n_{k,p,0} = c^n_{k,p,1}, c^n_{k,p,N_y+1} = c^n_{k,p,N_y},$$

$$c^n_{k,p,N_y+2} = c^n_{k,p,N_y-1}, \quad \text{for} \quad p = 1,\dots,N_x, c^n_{k,-1,q} = c^n_{k,2,q},$$

$$c^n_{k,0,q} = c^n_{k,1,q}, c^n_{k,N_x+1,q} = c^n_{k,N_x,q}, c^n_{k,N_x+2,q} = c^n_{k,N_x-1,q},$$

for $q = 1,\dots,N_y$.

Equation (3.1) can be arranged as

$$\begin{aligned}\frac{c^{n+1}_{k,p,q}}{\Delta t} &= \frac{c^n_{k,p,q}}{\Delta t} + \Delta_d((c^n_{k,p,q})^3 - 1.5c^n_{k,p,q}) \\ &\quad +0.5\Bigg(\frac{c^{n+1}_{k,p+1,q} - c^{n+1}_{k,p,q}}{h^2} - \frac{c^{n+1}_{k,p,q} - c^{n+1}_{k,p-1,q}}{h^2} \\ &\quad +\frac{c^{n+1}_{k,p,q+1} - c^{n+1}_{k,p,q}}{h^2} - \frac{c^{n+1}_{k,p,q} - c^{n+1}_{k,p,q-1}}{h^2}\Bigg) \\ &\quad -\frac{\epsilon^2}{h^2}\Bigg(\frac{c^{n+1}_{k,p+2,q} - c^{n+1}_{k,p+1,q}}{h^2} - \frac{c^{n+1}_{k,p+1,q} - c^{n+1}_{k,p,q}}{h^2} \\ &\quad +\frac{c^{n+1}_{k,p+1,q+1} - c^{n+1}_{k,p+1,q}}{h^2} - \frac{c^{n+1}_{k,p+1,q} - c^{n+1}_{k,p+1,q-1}}{h^2} \\ &\quad +\frac{c^{n+1}_{k,p,q} - c^{n+1}_{k,p-1,q}}{h^2} - \frac{c^{n+1}_{k,p-1,q} - c^{n+1}_{k,p-2,q}}{h^2} \\ &\quad +\frac{c^{n+1}_{k,p-1,q+1} - c^{n+1}_{k,p-1,q}}{h^2} - \frac{c^{n+1}_{k,p-1,q} - c^{n+1}_{k,p-1,q-1}}{h^2} \\ &\quad +\frac{c^{n+1}_{k,p+1,q+1} - c^{n+1}_{k,p,q+1}}{h^2} - \frac{c^{n+1}_{k,p,q+1} - c^{n+1}_{k,p-1,q+1}}{h^2} \\ &\quad +\frac{c^{n+1}_{k,p,q+2} - c^{n+1}_{k,p,q+1}}{h^2} - \frac{c^{n+1}_{k,p,q+1} - c^{n+1}_{k,p,q}}{h^2} \\ &\quad +\frac{c^{n+1}_{k,p+1,q-1} - c^{n+1}_{k,p,q-1}}{h^2} - \frac{c^{n+1}_{k,p,q-1} - c^{n+1}_{k,p-1,q-1}}{h^2} \\ &\quad +\frac{c^{n+1}_{k,p,q} - c^{n+1}_{k,p,q-1}}{h^2} - \frac{c^{n+1}_{k,p,q-1} - c^{n+1}_{k,p,q-2}}{h^2} \\ &\quad -4\Bigg(\frac{c^{n+1}_{k,p+1,q} - c^{n+1}_{k,p,q}}{h^2} - \frac{c^{n+1}_{k,p,q} - c^{n+1}_{k,p-1,q}}{h^2} \\ &\quad +\frac{c^{n+1}_{k,p,q+1} - c^{n+1}_{k,p,q}}{h^2} - \frac{c^{n+1}_{k,p,q} - c^{n+1}_{k,p,q-1}}{h^2}\Bigg)\Bigg) \\ &\quad +\Delta_d\beta(\mathbf{c}^n_{k,p,q}).\end{aligned} \tag{3.2}$$

In two-dimensional space, the ADE scheme has 8 different alternating direction loops. We describe one of the 8 loops with following example. By using the ADE scheme [19] to Eq (3.2), we have the following fully discrete form as follows:

$$\begin{aligned}\text{For } p &= 1,2,\dots,N_x \text{ and } q = 1,2,\dots,N_y, \\ \frac{c^*_{k,p,q}}{\Delta t} &= \frac{c^n_{k,p,q}}{\Delta t} + \Delta_d((c^n_{k,p,q})^3 - 1.5c^n_{k,p,q}) \\ &\quad +0.5\Bigg(\frac{c^n_{k,p+1,q} - c^n_{k,p,q}}{h^2} - \frac{c^*_{k,p,q} - c^*_{k,p-1,q}}{h^2} \\ &\quad +\frac{c^n_{k,p,q+1} - c^n_{k,p,q}}{h^2} - \frac{c^*_{k,p,q} - c^*_{k,p,q-1}}{h^2}\Bigg) \\ &\quad -\frac{\epsilon^2}{h^2}\Bigg(\frac{c^n_{k,p+2,q} - c^n_{k,p+1,q}}{h^2} - \frac{c^n_{k,p+1,q} - c^n_{k,p,q}}{h^2} \\ &\quad +\frac{c^n_{k,p+1,q+1} - c^n_{k,p+1,q}}{h^2} - \frac{c^n_{k,p+1,q} - c^n_{k,p+1,q-1}}{h^2} \\ &\quad +\frac{c^*_{k,p,q} - c^*_{k,p-1,q}}{h^2} - \frac{c^*_{k,p-1,q} - c^*_{k,p-2,q}}{h^2} \\ &\quad +\frac{c^*_{k,p-1,q+1} - c^*_{k,p-1,q}}{h^2} - \frac{c^*_{k,p-1,q} - c^*_{k,p-1,q-1}}{h^2}\end{aligned}$$

$$
\begin{aligned}
&+\frac{c^n_{k,p+1,q+1}-c^n_{k,p,q+1}}{h^2}-\frac{c^n_{k,p,q+1}-c^n_{k,p-1,q+1}}{h^2}\\
&+\frac{c^n_{k,p,q+2}-c^n_{k,p,q+1}}{h^2}-\frac{c^n_{k,p,q+1}-c^n_{k,p,q}}{h^2}\\
&+\frac{c^n_{k,p+1,q-1}-c^n_{k,p,q-1}}{h^2}-\frac{c^*_{k,p,q-1}-c^*_{k,p-1,q-1}}{h^2}\\
&+\frac{c^*_{k,p,q}-c^*_{k,p,q-1}}{h^2}-\frac{c^*_{k,p,q-1}-c^*_{k,p,q-2}}{h^2}\\
&-4\Bigg(\frac{c^n_{k,p+1,q}-c^n_{k,p,q}}{h^2}-\frac{c^*_{k,p,q}-c^*_{k,p-1,q}}{h^2}\\
&+\frac{c^n_{k,p,q+1}-c^n_{k,p,q}}{h^2}-\frac{c^*_{k,p,q}-c^*_{k,p,q-1}}{h^2}\Bigg)\Bigg)\\
&+\Delta_d\beta(\mathbf{c}^n_{k,p,q}). \qquad (3.3)
\end{aligned}
$$

Here, the discretization at time n and $n+1$ follows the definition of the first derivative, where the already updated values are assigned to time $n+1$, while the others remain at time n. The loops over p and q must be executed in the specified order, as the computations depend on the sequential update direction of values. We emphasize that a different directional loop order is applied at each time step. The numerical solution can be updated for $k = 1, 2$ using Eq (3.3) as follows:

$$
\begin{aligned}
\text{For } p &= 1, 2, \ldots, N_x \text{ and } q = 1, 2, \ldots, N_y,\\
c^*_{k,p,q} &= \frac{1}{R}\Bigg[\frac{c^n_{k,p,q}}{\Delta t}+\Delta_d((c^n_{k,p,q})^3-1.5c^n_{k,p,q})\\
&\quad+\frac{1}{2h^2}\Big(c^n_{k,p+1,q}+c^*_{k,p-1,q}-2c^n_{k,p,q}\Big)\\
&\quad+\frac{1}{2h^2}\Big(c^n_{k,p,q+1}+c^*_{k,p,q-1}\Big)\\
&\quad-\frac{\epsilon^2}{h^4}\Big[c^n_{k,p+2,q}+c^*_{k,p-2,q}+c^n_{k,p,q+2}+c^*_{k,p,q-2}\\
&\quad+c^n_{k,p+1,q-1}+c^*_{k,p-1,q-1}+2c^n_{k,p+1,q+1}\\
&\quad+2c^*_{k,p-1,q+1}+2c^*_{k,p-1,q-1}\\
&\quad-7c^*_{k,p-1,q}-c^n_{k,p-1,q}-8c^n_{k,p+1,q}-8c^n_{k,p,q+1}\\
&\quad-8c^*_{k,p,q-1}+10c^n_{k,p,q}\Big]+\Delta_d\beta(\mathbf{c}^n_{k,p,q})\Bigg],
\end{aligned}
$$

where $R = 1/\Delta t + 1/h^2 + 10\epsilon^2/h^4$. The other 7 nested loops are defined similarly. Because the ADE scheme does not satisfy conservation of the CH equation, we apply a previously developed mass correction process.

$$
c^{n+1}_{k,p,q} = c^*_{k,p,q}+\frac{\sum_{p,q}(c^0_{k,p,q}-c^*_{k,p,q})}{\sum_{p,q}\sqrt{F(c^*_{k,p,q})}}\sqrt{F(c^*_{k,p,q})}, \qquad (3.4)
$$

for $k = 1, 2$, where $F(c^{n+1}_{k,p,q}) = 0.25(c^{n+1}_{k,p,q})^2(c^{n+1}_{k,p,q}-1)^2$. Here, the mass correction process in (3.4) for mass conservation numerically demonstrates that mass is preserved through the following equation while maintaining the original interface profile.

$$
\begin{aligned}
\sum_{p,q}c^{n+1}_{k,p,q} &= \sum_{p,q}\left(c^*_{k,p,q}+\frac{\sum_{p,q}(c^0_{k,p,q}-c^*_{k,p,q})}{\sum_{p,q}\sqrt{F(c^*_{k,p,q})}}\sqrt{F(c^*_{k,p,q})}\right)\\
&= \sum_{p,q}c^*_{k,p,q}+\frac{\sum_{p,q}(c^0_{k,p,q}-c^*_{k,p,q})}{\sum_{p,q}\sqrt{F(c^*_{k,p,q})}}\sum_{p,q}\sqrt{F(c^*_{k,p,q})}\\
&= \sum_{p,q}c^0_{k,p,q}.
\end{aligned}
$$

Finally, the third component is updated using $c^{n+1}_{3,p,q} = 1 - c^{n+1}_{1,p,q} - c^{n+1}_{2,p,q}$.

Similarly, we describe the discrete computational scheme for the three-dimensional domain $\Omega = (L_x, R_x)\times(L_y, R_y)\times(L_z, R_z)$. Then, the domain is discretized into a cell centered domain $\Omega_h = \{(x_p = L_x+h(p-0.5),\ y_q = L_y+h(q-0.5),\ z_r = L_z + h(r-0.5))|1 \le p \le N_x,\ 1 \le q \le N_y,\ 1 \le r \le N_z\}$ with $c^n_{p,q,r}$ being the approximation of $c_k(x_p, y_q, z_r, n\Delta t)$. Assuming constant mobility, i.e. $M = 1$, we start with discretizing Eqs (2.1) and (2.2) using the linear convex splitting scheme:

$$
\begin{aligned}
\frac{c^{n+1}_{k,p,q,r}-c^n_{k,p,q,r}}{\Delta t} &= \Delta_d\Big[(c^n_{k,p,q,r})^3-\frac{3}{2}(c^n_{k,p,q,r})^2\Big]+\frac{1}{2}\Delta_d c^{n+1}_{k,p,q,r}\\
&\quad-\epsilon^2\Delta_d^2 c^{n+1}_{k,p,q,r}+\Delta_d\beta(\mathbf{c}^n_{k,p,q,r}), \qquad (3.5)
\end{aligned}
$$

where

$$
\beta(\mathbf{c}^n_{k,p,q,r}) = -\sum_{k=1}^{3}\Big[(c^n_{k,p,q,r})^3-1.5(c^n_{k,p,q,r})^2+0.5c^n_{k,p,q,r}\Big]/3.
$$

In three-dimensional domain, discrete Laplacian and biharmonic operators are defined as

$$
\begin{aligned}
\Delta_d c_{k,p,q,r} = (&c_{k,p+1,q,r}+c_{k,p-1,q,r}+c_{k,p,q+1,r}+c_{k,p,q-1,r}+\\
&c_{k,p,q,r+1}+c_{k,p,q,r-1}-6c_{k,p,q,r})/h^2
\end{aligned}
$$

and

$$
\Delta_d^2 c_{k,p,q,r} = \Delta_d(\Delta_d c_{k,p,q,r}),
$$

respectively.

The boundary conditions are defined in the same way:

$$\begin{aligned} c^n_{k,-1,q,r} &= c^n_{k,2,q,r}, \quad c^n_{k,0,q,r} = c^n_{k,1,q,r}, \\ c^n_{k,N_x+1,q,r} &= c^n_{k,N_x,q,r}, \quad c^n_{k,N_x+2,q,r} = c^n_{k,N_x-1,q,r}, \\ &\text{for } q = 1,\ldots,N_y \text{ and } r = 1,\ldots,N_z, \\ c^n_{k,p,-1,r} &= c^n_{k,p,2,r}, \quad c^n_{k,p,0,r} = c^n_{k,p,1,r}, \\ c^n_{k,p,N_y+1,r} &= c^n_{k,p,N_y,r}, \quad c^n_{k,p,N_y+2,r} = c^n_{k,p,N_y-1,r}, \\ &\text{for } p = 1,\ldots,N_x \text{ and } r = 1,\ldots,N_z, \\ c^n_{k,p,q,-1} &= c^n_{k,p,q,2}, \quad c^n_{k,p,q,0} = c^n_{k,p,q,1}, \\ c^n_{k,p,q,N_z+1} &= c^n_{k,p,q,N_z}, \quad c^n_{k,p,q,N_z+2} = c^n_{k,p,q,N_z-1}, \\ &\text{for } p = 1,\ldots,N_x \text{ and } q = 1,\ldots,N_y. \end{aligned}$$

We have introduced that the ADE scheme has 8 different cases of nested loops in two-dimensional space. In three dimensional space, it has 48 cases. Here, we present an example. Applying the ADE scheme [19, 28], the fully discrete form of Eq (3.5) for $k = 1, 2$ is given as follows:

$$\begin{aligned} &\text{For } p = 1,2,\ldots,N_x, \quad q = 1,2,\ldots,N_y, \quad r = 1,2,\ldots,N_z, \\ c^*_{k,p,q,r} =& \frac{1}{R}\Bigg[\frac{c^n_{k,p,q,r}}{\Delta t} + \Delta_d((c^n_{k,p,q,r})^3 - 1.5c^n_{k,p,q,r}) \\ &+ \frac{1}{2h^2}\Big(c^n_{k,p+1,q,r} + c^*_{k,p-1,q,r} + c^n_{k,p,q+1,r} + c^*_{k,p,q-1,r} \\ &+ c^n_{k,p,q,r+1} + c^*_{k,p,q,r-1} - 3c^n_{k,p,q,r}\Big) \\ &- \frac{\epsilon^2}{h^4}\Big[c^n_{k,p+2,q,r} + c^*_{k,p-2,q,r} + c^n_{k,p,q+2,r} + c^*_{k,p,q-2,r} \\ &+ c^n_{k,p,q,r+2} + c^*_{k,p,q,r-2} + c^n_{k,p+1,q-1,r} + c^*_{k,p+1,q-1,r} \\ &+ c^n_{k,p,q+1,r-1} + c^*_{k,p,q+1,r-1} + c^n_{k,p+1,q,r-1} + c^*_{k,p+1,q,r-1} \\ &+ 2\Big(c^n_{k,p+1,q+1,r} + c^*_{k,p-1,q+1,r} + c^*_{k,p-1,q-1,r} \\ &+ c^n_{k,p,q+1,r+1} + c^n_{k,p,q-1,r+1} + c^*_{k,p,q-1,r-1} \\ &+ c^n_{k,p+1,q,r+1} + c^*_{k,p-1,q,r} + c^*_{k,p-1,q,r-1}\Big) \\ &- 2c^n_{k,p-1,q,r} - 10c^*_{k,p-1,q,r} - c^n_{k,p,q-1,r} - 11c^*_{k,p,q-1,r} \\ &- 12\Big(c^n_{k,p+1,q,r} + c^n_{k,p,q+1,r} + c^n_{k,p,q,r+1} + c^*_{k,p,q,r-1}\Big) \\ &+ 21c^n_{k,p,q,r}\Big] + \Delta_d\beta(\mathfrak{c}^n_{k,p,q,r})\Bigg], \end{aligned} \tag{3.6}$$

where $R = 1/\Delta t + 3/2h^2 + 21\epsilon^2/h^4$. The loops over p and q must be executed in the specified order, as the computations depend on the sequential update direction of values. The other 47 cases are defined in the same way. We emphasize that a different directional loop order is applied at each time step. Saul'yev-type scheme does not satisfy mass conservation of the CH equation. Therefore, we apply a previously developed mass correction process to achieve mass conservation:

$$c^{n+1}_{k,p,q,r} = c^*_{k,p,q,r} + \frac{\sum_{p,q,r}(c^0_{k,p,q,r} - c^*_{k,p,q,r})}{\sum_{p,q,r}\sqrt{F(c^*_{k,p,q,r})}}\sqrt{F(c^*_{k,p,q,r})}, \tag{3.7}$$

for $k = 1, 2$, where $F(c^*_{k,p,q,r}) = 0.25(c^*_{k,p,q,r})^2(c^*_{k,p,q,r} - 1)^2$. Here, the mass correction process in (3.7) for mass conservation demonstrates numerically that mass is conserved through the following equation.

$$\begin{aligned} &\sum_{p,q,r} c^{n+1}_{k,p,q,r} \\ &= \sum_{p,q,r}\left(c^*_{k,p,q,r} + \frac{\sum_{p,q,r}(c^0_{k,p,q,r} - c^*_{k,p,q,r})}{\sum_{p,q,r}\sqrt{F(c^*_{k,p,q,r})}}\sqrt{F(c^*_{k,p,q,r})}\right) \\ &= \sum_{p,q,r} c^*_{k,p,q,r} + \frac{\sum_{p,q,r}(c^0_{k,p,q,r} - c^*_{k,p,q,r})}{\sum_{p,q,r}\sqrt{F(c^*_{k,p,q,r})}}\sum_{p,q,r}\sqrt{F(c^*_{k,p,q,r})} \\ &= \sum_{p,q,r} c^0_{k,p,q,r}. \end{aligned}$$

Finally, the third component is updated using

$$c^{n+1}_{3,p,q,r} = 1 - c^{n+1}_{1,p,q,r} - c^{n+1}_{2,p,q,r}.$$

4. Computational tests

Now, we conduct several computational experiments for the ternary CH system using the proposed ADE method on two- and three-dimensional spaces. We consider the phase separation and liquid lens dynamics within the ternary CH system. From the equilibrium profile of the CH equation, the distance over which the concentration field varies from 0.05 to 0.95 is approximately $4\sqrt{2}\tanh^{-1}(0.9)$. Therefore, we take interfacial thickness control parameter ϵ as $\epsilon_m = hm/[4\sqrt{2}\tanh^{-1}(0.9)]$ to ensure that the distance of the interface spans m grid points [29].

4.1. Two-dimensional space

We present the performance of the proposed algorithm for the ternary CH system by adopting various numerical experiments such as ternary phase separation and liquid lens. We consider the ternary CH system on two-dimensional

computational domain $(0,1)\times(0,1)$ with uniform grid $N_x = N_y = 128$ and $h = 1/128$. We take time step size as $\Delta t = 0.5h^2$ and interfacial parameter as $\epsilon = \epsilon_4$. First, we investigate the phase evolutions of the ternary CH system with the following random initial conditions with random permutation of the integers r_1 and r_2, and r_3 from 1 to 3: $[r_1\ r_2\ r_3]$ = randperm(3) for $1 \le p \le N_x$, $1 \le q \le N_y$.

$$\begin{aligned} c^0_{r_1,p,q} &= \text{rand}_{1,p,q}, \\ c^0_{r_2,p,q} &= (1 - c_{r_1,p,q})\text{rand}_{2,p,q}, \\ c^0_{r_3,p,q} &= 1 - c^0_{r_1,p,q} - c^0_{r_2,p,q}, \end{aligned} \tag{4.1}$$

where $\text{rand}_{1,p,q}$ and $\text{rand}_{2,p,q}$ are uniform random numbers between 0 and 1.

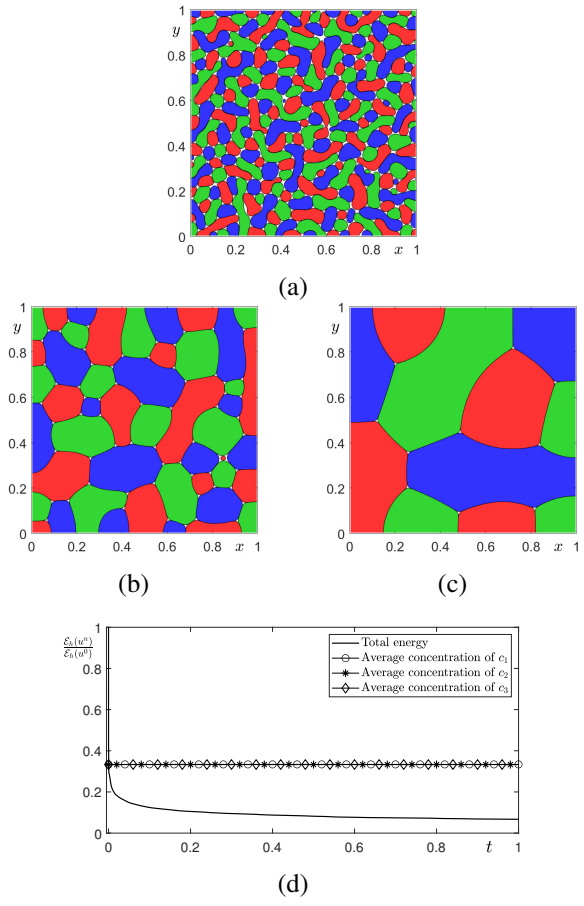

Figure 1. Temporal evolutions of the ternary CH system, where c_1, c_2, and c_3 are represented as filled contours at level 0.5 in red, green, and blue, respectively. (a), (b), and (c) are snapshots at $t = 0.0122$, 0.6104, and 15.2588, respectively. (d) Temporal evolution of the discrete total energy and average concentrations.

In Figure 1(a)–(c), the snapshots of the ternary phase separation for the ternary CH system are illustrated. Here, c_1, c_2, and c_3 are represented as filled contours at level 0.5 in red, green, and blue, respectively. Figure 1(d) shows the time evolution of the discrete total energy and average concentrations for c_1, c_2, and c_3. We can observe that the total energy decreases and the average concentrations are constant. In two-dimensional space, discrete total energy is defined as follows:

$$\begin{aligned} \mathcal{E}_h(\mathbf{c}^n) = \sum_{k=1}^{3}\Bigg[& h^2 \sum_{p=1}^{N_x}\sum_{q=1}^{N_y} F(c^n_{k,p,q}) + \frac{\epsilon^2}{2}\sum_{q=1}^{N_y}\Bigg((c^n_{k,1,q} - c^n_{k,0,q})^2 \\ & + \sum_{p=1}^{N_x-1}(c^n_{k,p+1,q} - c^n_{k,p,q})^2 + (c^n_{k,N_x+1,q} - c^n_{k,N_x,q})^2\Bigg) \\ & + \frac{\epsilon^2}{2}\sum_{p=1}^{N_x}\Bigg((c^n_{k,p,1} - c^n_{k,p,0})^2 + \sum_{q=1}^{N_y-1}(c^n_{k,p,q+1} - c^n_{k,p,q})^2 \\ & + (c^n_{k,p,N_y+1} - c^n_{k,p,N_y})^2\Bigg)\Bigg]. \end{aligned}$$

To validate the practical stability of the proposed numerical algorithm, we compare the maximum stable time step size $\Delta t_{\max}$, between the fully explicit method and the proposed method for various mesh sizes $h = 1/16$, $1/32$, $1/64$, and $1/128$ under the given random initial condition (4.1). First, we define the numerical solution as stable if it satisfies the following condition. $-0.2 < c^{n+1}_{k,p,q} < 1.2$ for $p = 1,\ldots,N_x$, $q = 1,\ldots,N_y$, $k = 1,2,3$. Next, to determine the maximum stable time step, we begin with an initial time step size of $\Delta t = 0.1h^2$ and increment Δt by $h^2 \times 1.0e\text{-}8$. If the numerical solution stays stable for 500 iterations, we consider the corresponding Δt a stable time step size, incrementing Δt again by $h^2 \times 1.0e\text{-}8$. Consequently, when Δt first leads to an unstable numerical solution within 500 iterations, the maximum stable time step size $\Delta t_{\max}$ is defined as $\Delta t - h^2 \times 1.0e\text{-}8$. Table 1 lists $\Delta t_{\max}$ for the proposed and the fully explicit methods with various mesh sizes. It can be observed that the maximum time step size of the proposed method is significantly larger than that of the fully explicit method.

Next, we consider a spreading of a rectangular liquid lens on the unit computational domain $(0,1)\times(0,1)$ with various interfacial parameters $\epsilon = \epsilon_2$, ϵ_4, and ϵ_9. The rectangular liquid lens (c_2) is located at the center of the domain,

between two fluids c_1 and c_3. The initial condition for the liquid lens is illustrated in the first column of Figure 2(a). Figure 2 shows the temporal evolution of a liquid lens with a rectangular liquid lens for the ternary CH system until $t = 3.8147$ for various interfacial parameters ϵ. From the results in Figure 2, when ϵ is too small (e.g., $\epsilon = \epsilon_2$), the numerical solution is pinned and does not evolve. Conversely, when ϵ is too large (e.g., $\epsilon = \epsilon_9$), the vacuum phenomenon at the triple junction becomes significant, and as a result, the numerical solution spreads.

To simulate phase separation of the ternary CH system using the proposed scheme, the initial conditions are set to stiff u-shape as seen in Figure 3(a). The temporal evolutions of the ternary CH system can be seen in Figure 3(b)–(d). At final time $t = 12.4359$, the phase separation is well performed using the proposed scheme.

The main advantage of the proposed ADE method lies in its implicit formulation, which allows for explicit computations while maintaining numerical stability. Traditional implicit or semi-implicit methods often involve significant computational complexity, making them challenging to apply to problems in complex domains. In contrast, the proposed ADE method offers a simpler computational approach, making it more convenient and efficient for solving problems in such domains. Figure 4 shows the temporal evolutions of the ternary CH system with randomly perturbed initial condition in a complex domain. Phase separation of the ternary CH system can be observed even in a complex domain. Here, we use the parameters as $h = 1/150$, $\Delta t = h^2$, and $\epsilon = \epsilon_4$.

To study the accuracy of the proposed method for the ternary CH system, we conduct convergence tests for both time and space using reference solutions [30]. We set the initial condition

$$
\begin{aligned}
c_1(\mathbf{x},0) =& \frac{1}{8}\Big[\tanh\Big(\frac{x-1/3}{0.02\sqrt{2}}\Big)+1\Big]-\frac{1}{4}\Big[\tanh\Big(\frac{x-1/3}{0.02\sqrt{2}}\Big)-1\Big],\\
c_2(\mathbf{x},0) =& \frac{1}{8}\Big[\tanh\Big(\frac{x-2/3}{0.02\sqrt{2}}\Big)+1\Big]-\frac{1}{4}\Big[\tanh\Big(\frac{x-2/3}{0.02\sqrt{2}}\Big)-1\Big]\\
&+\frac{1}{8}\Big[\tanh\Big(\frac{x-1/3}{0.02\sqrt{2}}\Big)-1\Big],\\
c_3(\mathbf{x},0) =& 1-c_1(\mathbf{x},0)-c_2(\mathbf{x},0),
\end{aligned}
$$

on $\Omega = (0,1)\times(0,0.1)$. For the temporal convergence analysis, we set $h = 1/150$, $\epsilon = 4h/(4\sqrt{2}\tanh^{-1}(0.9))$. Since the analytic solution is hard to find, we use high-resolution reference solution [31] by using the time step $\Delta t_{\text{ref}} = 2^{-20}$. We note that a manufactured solution may be used as a reference solution [32]. We use increasingly coarser time steps $\Delta t = 32\Delta t_{\text{ref}}$, $64\Delta t_{\text{ref}}$, and $128\Delta t_{\text{ref}}$. The test is conducted until $t = 2^{-13}$. Table 2 lists l_2-errors and convergence rates for time. As demonstrated, the proposed scheme maintains first-order temporal accuracy.

For the spatial convergence analysis, we fix the time step size $\Delta t = 10^{-8}$. We take high resolution reference solution by using mesh size $h = 4\times10^{-4}$ [33]. We use increasingly fine grids $h = 1/20$, $h = 1/40$, and $h = 1/80$. The convergence test is conducted until $t = 10^{-6}$. Table 3 lists l_2-errors and convergence rates for space. Since the central difference method is used for the spatial discretization, it can be confirmed that the proposed algorithm achieves second-order accuracy in space.

Finally, we measure the CPU time for progressively larger-scale simulations to demonstrate the temporal efficiency and memory usage of the proposed method. The test is conducted with a fixed step size $h = 1/100$ and a time step size $\Delta t = h^2$, on computational domains of increasing scale: $(0,1)^2, (0,2)^2, (0,3)^2, (0,4)^2, (0,5)^2$, and $(0,6)^2$ over 2000 iterations. For the test, the randomly perturbed initial conditions in Eq (4.1) are used to measure CPU time for the simulation. Figure 5 illustrates the relation between CPU time and the number of grid points for the proposed method. The circles correspond to the numerical results from the experiment, while the dashed red line is a linear fitted line for these results. This linear relationship suggests that the CPU time increases almost proportionally with the number of grid points and indicates a typical computational cost scaling in numerical simulations.

Table 1. Maximum time step $\Delta t_{\max}$ ensuring stable computation for the proposed method and fully explicit method.

Mesh size h	1/16	1/32	1/64	1/128
Proposed method (a)	2.5539×10^{-2}	4.2315×10^{-3}	1.1750×10^{-3}	1.6815×10^{-4}
Fully explicit method (b)	4.9762×10^{-4}	1.2419×10^{-4}	3.1470×10^{-5}	7.8070×10^{-6}
Ratio (a/b)	51.3223	34.0728	37.3371	21.5384

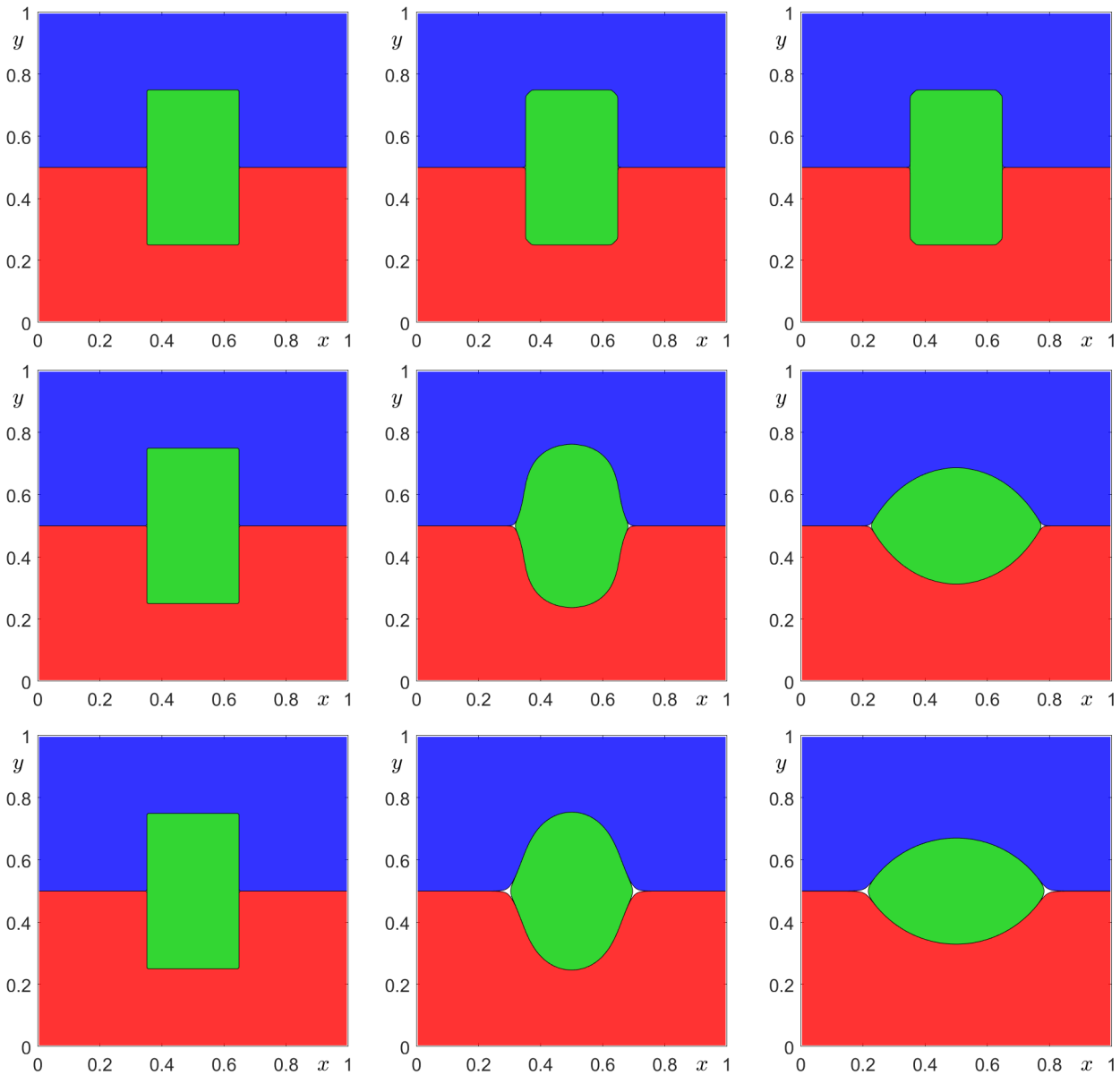

Figure 2. Temporal evolution of liquid lens with various interfacial parameters. From top to bottom row, the interfacial parameters are $\epsilon = \epsilon_2$, ϵ_4, and ϵ_9. The times shown are (a) $t = 0$, (b) $t = 0.2441$, and (c) $t = 3.8147$. Here, c_1, c_2, and c_3 are represented as filled contours at level 0.5 in red, green, and blue, respectively.

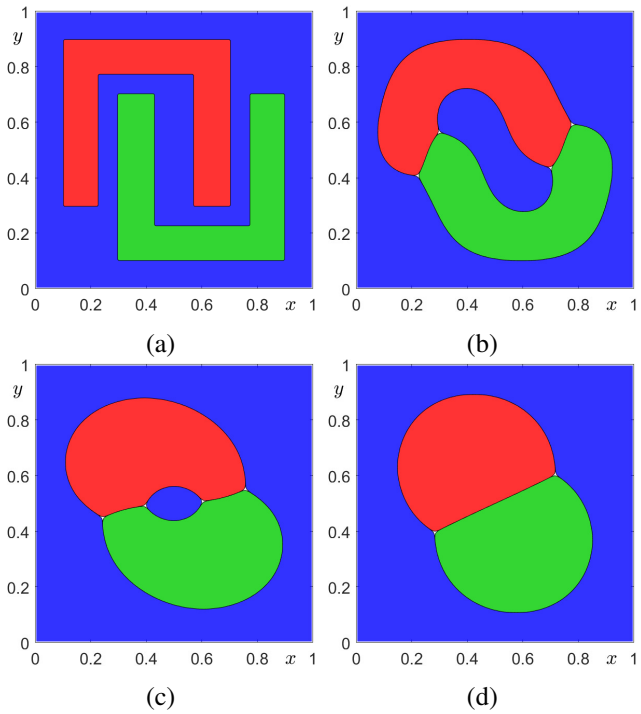

Figure 3. Temporal evolutions of the ternary CH system, where c_1, c_2, and c_3 are represented as filled contours at level 0.5 in red, green, and blue, respectively. The times corresponding to (a)–(e) are $t = 0$, 1.2970, 3.8147, and 12.4359, respectively.

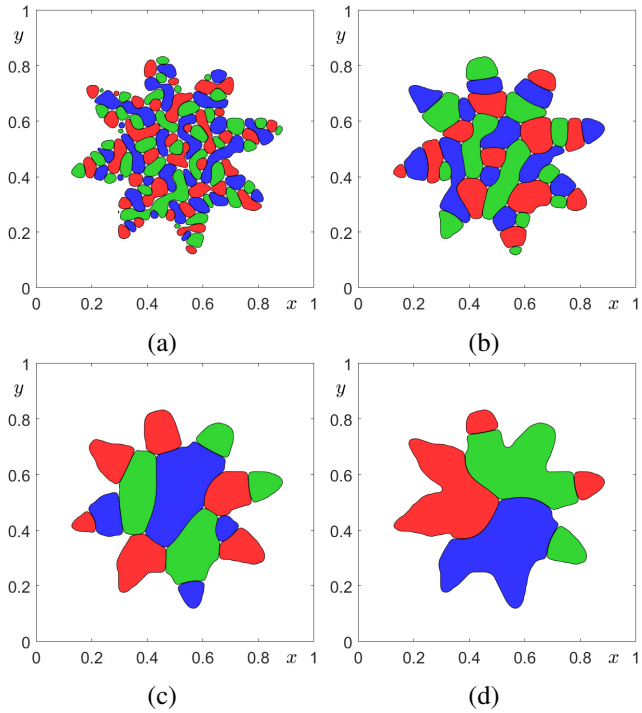

Figure 4. On a complex domain, temporal evolutions of the ternary CH system with randomly perturbed initial condition, where c_1, c_2, and c_3 are represented as filled contours at level 0.5 in red, green, and blue, respectively. The times corresponding to (a)–(e) are $t = 0.0089$, 0.0889, 0.4978, and 19.9911, respectively.

Table 2. Temporal errors and convergence rates.

Δt	$128\Delta t_{\text{ref}}$	$64\Delta t_{\text{ref}}$	$32\Delta t_{\text{ref}}$
l_2-error	0.0712×10^{-5}	0.1656×10^{-5}	0.3331×10^{-5}
rate		1.2186	1.0079

Table 3. Spatial errors and convergence rates.

h	1/20	1/40	1/80
l_2-error	1.589×10^{-7}	3.235×10^{-8}	7.0164×10^{-9}
rate		2.2963	2.2050

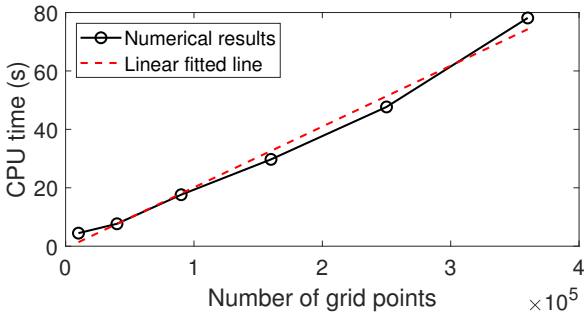

Figure 5. CPU time with respect to the number of grid points. The circles represent the numerical results, and the dashed line is the linear fit.

4.2. Three-dimensional space

We investigate the phase evolutions of the ternary CH system with the following random initial conditions with random permutation of the integers r_1, r_2, and r_3 from 1 to 3: $[r_1\ r_2\ r_3]$ = randperm(3) for $1 \le p \le N_x$, $1 \le q \le N_y$, $1 \le r \le N_z$.

$$c^0_{r_1,p,q,r} = \text{rand}_{1,p,q,r},\ c^0_{r_2,p,q,r} = (1 - c_{r_1,p,q,r})\text{rand}_{2,p,q,r},$$

$$c^0_{r_3,p,q,r} = 1 - c^0_{r_1,p,q,r} - c^0_{r_2,p,q,r},$$

where $\text{rand}_{1,p,q,r}$ and $\text{rand}_{2,p,q,r}$ are uniform random numbers between 0 and 1. Here, we use $\epsilon = \epsilon_4$, $h = 1/64$ and $\Delta t = 0.2h^2$.

The temporal evolutions of the ternary CH system with random perturbed initial condition can be seen in Figure 6. In Figure 6, c_1, c_2, and c_3 are represented as isosurfaces at 0.5 level in black, dark gray, and light gray, respectively. We can note the coarser phase separation occurring at t = 1.0758, which differs from the finer state observed at t = 0.0211. In a three-dimensional unit domain, we consider the spreading of a cuboid liquid lens on the unit computational domain $(0, 1) \times (0, 1) \times (0, 1)$. The cuboid liquid lens (c_2) is located at the center of the domain, between two fluids, c_1 and c_3. The initial condition is illustrated in Figure 7(a). Here, we use $\epsilon = \epsilon_4$, $h = 1/64$ and $\Delta t = 0.1h^2$.

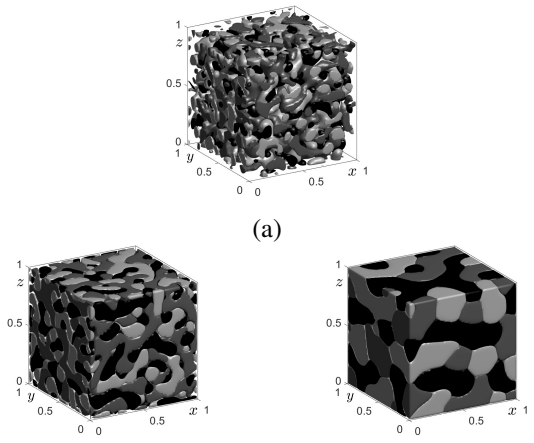

(a) (b) (c)

Figure 6. Temporal evolutions of a three-dimensional ternary CH system, where c_1, c_2, and c_3 are represented as isosurfaces at the 0.5 level in black, dark gray, and light gray, respectively. The times corresponding to (a)–(c) are t = 0.0211, 0.0352, and 1.0758, respectively.

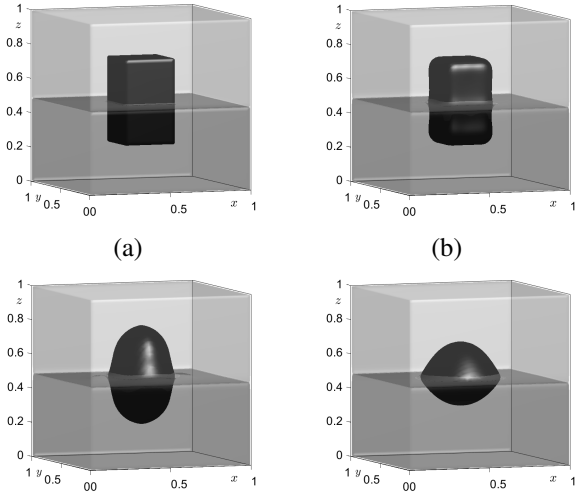

(a) (b) (c) (d)

Figure 7. Temporal evolution of a three-dimensional liquid lens at (a) $t = 0$, (b) $t = 0.0059$, (c) $t = 0.1430$, and (d) $t = 0.8156$. Here, c_1, c_2, and c_3 are represented as isosurfaces at the 0.5 level in light gray, black, and dark gray, respectively.

5. Conclusions

In this article, we have successfully overcome the challenge of numerically solving the ternary CH system, which includes fourth-order nonlinear terms, by using a highly practical and stable explicit FDM. The proposed method not only offers simplicity of implementation but also ensures numerical stability. Therefore, we can use larger time steps and significantly reduce the computational cost. Through a series of computational experiments, we have demonstrated the improved performance of the proposed FDM over a fully explicit Euler-type method. We expect that our work will inspire further investigations and advancements in numerical methods for multi-component systems.

Use of Generative-AI tools declaration

This article was not created using Artificial Intelligence (AI) tools.

Acknowledgments

Hyundong Kim was supported by Basic Science Research Program through the National Research Foundation of Korea(NRF) funded by the Ministry of Education (2021R1A6A1A03044326). The corresponding author (J.S. Kim) was supported by the Brain Korea 21 FOUR (BK 21 FOUR) from the Ministry of Education of Korea. The authors would like to express their sincere gratitude to the reviewers for their constructive comments and suggestions, which significantly improved the quality of this manuscript.

Conflicts of interest

All authors declare that there are no conflicts of interest in this paper.

References

1. J. E. Morral, J. W. Cahn, Spinodal decomposition in ternary systems, *Acta Metall. Sinica*, **19** (1971), 1037–1045. https://doi.org/10.1016/0001-6160(71)90036-8
2. S. Bhattacharyya, T. A. Abinandanan, A study of phase separation in ternary alloys, *Bull. Mater. Sci.*, **26** (2003), 193–197. https://doi.org/10.1007/BF02712812
3. S. Sugathan, S. Bhattacharya, A phase-field study of elastic stress effects on phase separation in ternary alloys, *Comput. Mater. Sci.*, **172** (2020), 109284. https://doi.org/10.1016/j.commatsci.2019.109284
4. G. I. T*ó*th, M. Zarifi, B. Kvamme, Phase-field theory of multicomponent incompressible Cahn–Hilliard liquids, *Phys. Rev. E*, **93** (2016), 013126. https://doi.org/10.1103/PhysRevE.93.013126
5. J. M. Park, Mathematical modeling and computational simulation of phase separation in ternary mixtures, *Appl. Math. Comput.*, **330** (2018), 11–22. https://doi.org/10.1016/j.amc.2018.02.006
6. H. G. Lee, J. Shin, J. Y. Lee, A high-order convex splitting method for a non-additive Cahn–Hilliard energy functional, *Mathematics*, **7** (2019), 1242. https://doi.org/10.3390/math7121242
7. W. Chen, C. Wang, S. Wang, X. Wang, S. M. Wise, Energy stable numerical schemes for ternary Cahn–Hilliard system, *J. Sci. Comput.*, **84** (2020), 1–36. https://doi.org/10.1007/s10915-020-01276-z
8. C. Chen, X. Li, J. Zhang, X. Yang, Efficient linear, decoupled, and unconditionally stable scheme for a ternary Cahn–Hilliard type Nakazawa-Ohta phase-field model for tri-block copolymers, *Appl. Math. Comput.*, **388** (2021), 125463. https://doi.org/10.1016/j.amc.2020.125463
9. L. Dong, C. Wang, S. M. Wise, Z. Zhang, A positivity-preserving, energy stable scheme for a ternary Cahn–Hilliard system with the singular interfacial parameters, *J. Comput. Phys.*, **442** (2021), 110451. https://doi.org/10.1016/j.jcp.2021.110451
10. Z. Wang, J. Zhang, X. Yang, Decoupled, second-order accurate in time and unconditionally energy stable scheme for a hydrodynamically coupled ternary Cahn–Hilliard phase-field model of triblock copolymer melts, *Comput. Math. Appl.*, **124** (2022), 241–257. https://doi.org/10.1016/j.camwa.2022.08.046
11. C. Rohde, L. von Wolff, A ternary Cahn-Hilliard-Navier-Stokes model for two-phase flow with precipitation and dissolution, *Math. Mod. Methods Appl. Sci.*, **31** (2021), 1–35. https://doi.org/10.1142/S0218202521500019
12. C. Zhan, Z. Chai, B. Shi, A ternary phase-field model for two-phase flows in complex geometries, *Phys. D*, **460** (2024), 134087. https://doi.org/10.1016/j.physd.2024.134087
13. J. Manzanero, C. Redondo, G. Rubio, E. Ferrer, *Á*. Rivero–Jim*é*nez, A discontinuous Galerkin approximation for a wall-bounded consistent three-component Cahn–Hilliard flow model, *Comput. Fluids*, **225** (2021), 104971. https://doi.org/10.1016/j.compfluid.2021.104971
14. M. Rudziva, O. A. Noreldin, P. Sibanda, S. P. Goqo, A bifurcation analysis of multicomponent convection in a rotating low prandtl number fluid with internal heating, *Appl. Comput. Math.*, **21** (2022), 78–100. https://doi.org/10.30546/1683-6154.21.1.2022.78
15. C. G. Gal, M. Grasselli, A. Poiatti, J. L. Shomberg, Multi–component Cahn–Hilliard systems with singular potentials: theoretical results, *Appl. Math. Optim.*, **88** (2023), 73. https://doi.org/10.1007/s00245-023-10048-8

16. S. Zhou, Y. M. Xie, Numerical simulation of three-dimensional multicomponent Cahn–Hilliard systems, *Int. J. Mech. Sci.*, **198** (2021), 106349. https://doi.org/10.1016/j.ijmecsci.2021.106349

17. Y. Li, R. Liu, Q. Xia, C. He, Z. Li, First-and second-order unconditionally stable direct discretization methods for multi-component Cahn–Hilliard system on surfaces, *J. Comput. Appl. Math.*, **401** (2022), 113778. https://doi.org/10.1016/j.cam.2021.113778

18. V. K. Saul'yev, *Integration of equations of parabolic type by the method of nets*, New York: Pergamon Press, 1964. https://doi.org/10.1016/C2013-0-01754-9

19. V. K. Saul'yev, A method of numerical integration of diffusion equations, *Dokl. Akad. Nauk*, **115** (1957), 1077–1079.

20. L. J. Campbell, B. Yin, On the stability of alternating direction explicit methods for advection diffusion equations, *Numer. Methods Part. Differ. Equations*, **23** (2007), 1429–1444. https://doi.org/10.1002/num.20233

21. X. Yang, W. Zhao, W. Zhao, Optimal error estimates of a discontinuous Galerkin method for stochastic Allen–Cahn equation driven by multiplicative noise, *Commun. Comput. Phys.*, **36** (2024), 133–159. https://doi.org/10.4208/cicp.OA-2023-0280

22. K. K. Hasanov, T. M. Gasumov, Minimal energy control for the wave equation with non-classical boundary condition, *Appl. Comput. Math.*, **9** (2010), 47–56.

23. A. Ashyralyev, A. Erdogan, S. Tekalan, An investigation on finite difference method for the first order partial differential equation with the nonlocal boundary condition, *Appl. Comput. Math.*, **18** (2019), 247–260.

24. M. Shen, B. Q. Li, Bubble rising and interaction in ternary fluid flow: a phase field study, *RSC Adv.*, **13** (2023), 3561–3574. https://doi.org/10.1039/D2RA06144A

25. G. Lee, S. Lee, Study on decoupled projection method for Cahn–Hilliard equation, *J. Korean Soc. Ind. Appl. Math.*, **27** (2023), 272–280. https://doi.org/10.12941/jksiam.2023.27.272

26. D. J. Eyre, An unconditionally stable one-step scheme for gradient systems, Unpublished article, 1997.

27. J. Yang, Z. Tan, J. Kim, Original variables based energy-stable time-dependent auxiliary variable method for the incompressible Navier–Stokes equation, *Comput. Fluids*, **240** (2022), 105432. https://doi.org/10.1016/j.compfluid.2022.105432

28. H. Kim, C. Lee, S. Yoon, Y. Choi, J. Kim, A fast shape transformation using a phase-field model, *Extreme Mech. Lett.*, **52** (2022), 101633. https://doi.org/10.1016/j.eml.2022.101633

29. S. Ham, Y. Li, D. Jeong, C. Lee, S. Kwak, Y. Hwang, et al., An explicit adaptive finite difference method for the Cahn–Hilliard equation, *J. Nonlinear Sci.*, **32** (2022), 80. https://doi.org/10.1007/s00332-022-09844-3

30. J. Yang, J. Kim, Efficient and structure-preserving time-dependent auxiliary variable method for a conservative Allen–Cahn type surfactant system, *Eng. Comput.*, **38** (2022), 5231–5250. https://doi.org/10.1007/s00366-021-01583-5

31. S. Lee, S. Yoon, C. Lee, S. Kim, H. Kim, J. Yang, et al., Effective time step analysis for the Allen–Cahn equation with a high-order polynomial free energy, *Int. J. Numer. Methods Eng.*, **123** (2022), 4726–4743. https://doi.org/10.1002/nme.7053

32. Y. Hwang, C. Lee, S. Kwak, Y. Choi, S. Ham, S. Kang, et al., Benchmark problems for the numerical schemes of the phase-field equations, *Discrete Dyn. Nat. Soc.*, **2022** (2022), 2751592. https://doi.org/10.1155/2022/2751592

33. C. Lee, S. Yoon, J. Park, H. Kim, Y. Li, D. Jeong, et al., Phase-field computations of anisotropic ice crystal growth on a spherical surface, *Comput. Math. Appl.,* **125** (2022), 25–33. https://doi.org/10.1016/j.camwa.2022.08.035

AIMS Press